Towing Asteroids with Gravity Tractors Enhanced by Tethers and Solar Sails

Haijun Shen* and Carlos M. Roithmayr†

Material collected from an asteroid's surface can be used to increase gravitational attraction between the asteroid and a Gravity Tractor (GT); the spacecraft therefore operates more effectively and is referred to as an Enhanced Gravity Tractor (EGT). The use of tethers and solar sails to further improve effectiveness and simplify operations is investigated. By employing a tether, the asteroidal material can be placed close to the asteroid while the spacecraft is stationed farther away, resulting in a better safety margin and improved thruster efficiency. A solar sail on a spacecraft can naturally provide radial offset and inter-spacecraft separation required for multiple EGTs.

I. Introduction

Collisions between objects that make up our solar system are commonplace, as evidenced by numerous craters on planets, moons, asteroids, and comets. In fact, it has been theorized that most of the boulders and regolith on asteroids such as 21 Lutetia, 433 Eros, etc., are formed by such collisions.[1–3] The planet Earth is not immune from the danger. Even though our atmosphere protects the Earth by incinerating smaller objects (sub 10-m range) before they reach the surface, larger objects can survive the atmospheric transit and cause catastrophic damage.

The extinction of the dinosaurs and many other species is attributed to a huge asteroid, more than 10 km in diameter, that hit the Yucatan Peninsula in Mexico sixty-five million years ago. In 1908, Tunguska, Siberia was devastated by a small object roughly 50 meters across. Although it exploded in the air before it hit the ground, it nevertheless flattened 60 million trees. It would have erased St. Petersburg had it arrived four hours and fifty-two minutes later.[4] More recently, the 300-m asteroid 1989 FC missed the Earth by merely six hours on March 23rd, 1989.[5] An impact in the ocean from an asteroid of this size can cause a tsunami with 300 times more energy than the one caused by the 2004 Sumatra-Andaman earthquake, which killed 200,000 people.[6] On February 15th, 2013, the Chelyabinsk meteor survived atmospheric transit and exploded in an air burst at a height of roughly 29.7 km, creating many small meteorites that reached the ground. The airburst released a total kinetic energy that was 20–30 times the amount produced by the atomic bomb detonated at Hiroshima. Even though most of the energy was absorbed by the atmosphere, it caused infrastructure damage and seriously injured as many as 1,500 people.[7]

The threat is real, and the best conceivable mitigation consists of detecting and deflecting potentially hazardous objects. Various ways of deflecting an asteroid have been proposed. High-energy schemes utilizing kinetic impactors[8–10] and nuclear or non-nuclear blasts[11] are capable of achieving large deflection in a short period of time, which is effective if a threat is detected with a short warning time. These schemes are not suitable for rubble-pile asteroids held together by weak gravity and cohesion. For smaller asteroids with a long warning time, a few low-energy schemes have been proposed. In Ref. [12], Bombardelli and Pelaez suggest blasting an asteroid surface with ion beams, which transfers momentum from the ion particles to the asteroid.

Mechanical attachment of a propulsion system to an asteroid is problematic. First, it may be difficult to obtain firm attachment if the asteroid is a rubble pile or composed of low-strength material. Second, an asteroid's rotational motion interferes with application of thrust in the best direction for deflection. These problems are solved with a concept proposed by Lu and Love in Ref. [13]; it involves no physical contact and is known as the Gravity Tractor (GT). A spacecraft is placed so that it leads the asteroid in its heliocentric trajectory. Two thrusters impart momentum to the spacecraft, which tugs the asteroid through mutual gravitational attraction. The thrusters are canted in order to prevent impingement of the plume streams on the asteroid surface. However, the portion of thrust that contributes to effective asteroid deflection is proportional to the cosine of the cant angle; wasted thrust is proportional to the sine

*Analytical Mechanics Associates, Inc., 21 Enterprise Parkway, Suite 300, Hampton, VA 23666, USA +1 757 865 0000, shen@ama-inc.com

†NASA Langley Research Center, Vehicle Analysis Branch, MS 451, 1 North Dryden Street, Hampton, VA, 23681, USA +1 757 864 6778, carlos.m.roithmayr@nasa.gov

of the cant angle. The disadvantage of thruster cant is addressed by McInnes in Ref. [14] by placing the spacecraft in a halo orbit in front of the asteroid. A properly sized halo orbit makes it possible to prevent plume impingement without canting the thrusters. This idea is extended by Wie in Ref. [15] to include multiple spacecraft in a halo orbit to expedite deflection. Another innovation introduced in Ref. [15] is the addition of a solar sail to the gravity tractor. The sail is oriented so as to provide a component of Solar Radiation Pressure (SRP) force in the direction of the asteroid's motion and impart momentum to the asteroid-spacecraft system.

A gravity tractor can be made more effective by adding mass to the spacecraft because doing so increases the gravitational attraction between the asteroid and the spacecraft. Collecting boulders and regolith from the asteroid surface is an attractive way to add mass to the spacecraft.[16,17] In-situ utilization of native asteroidal material reduces the launch cost and trip time associated with sending the same amount of mass from Earth. Compared to regular GT operations without the additional mass, the Enhanced Gravity Tractor (EGT) is more effective, and thus, requires less time to achieve the same amount of deflection. Reference [17] shows that the deflection times can be reduced by a factor of 10 to 50 or more with EGT compared to GT, depending on the propulsion system's capability and the mass collected.

In this paper we explore the use of a tether and a solar sail to make an EGT more effective and provide operational simplification. A container of asteroidal material is attached to a tether and placed close to the asteroid to increase gravitational attraction, while the spacecraft is placed farther away from the asteroid for a better margin of safety. In the case of a single EGT placed in front of the asteroid, as in Ref. [13], the increased distance afforded by a tether permits a smaller thruster cant angle. Operationally, the halo orbit employed in Ref. [14] requires tight orbit control. Instead of using a halo orbit to provide lateral displacement of the spacecraft, we employ a solar sail. In the case of a single spacecraft placed in the asteroid's heliocentric orbit plane and slightly farther away from the sun than the asteroid, as in Ref. [15], the cant angle of the towing thrusters can be eliminated. The solar sail can be oriented so that it provides only the lateral displacement, or so that it also provides some of the towing force. Two additional spacecraft with solar sails can be placed to either side of the asteroid's heliocentric orbit plane; in this case, their solar sails can be oriented so as to maintain the out-of-plane positions.

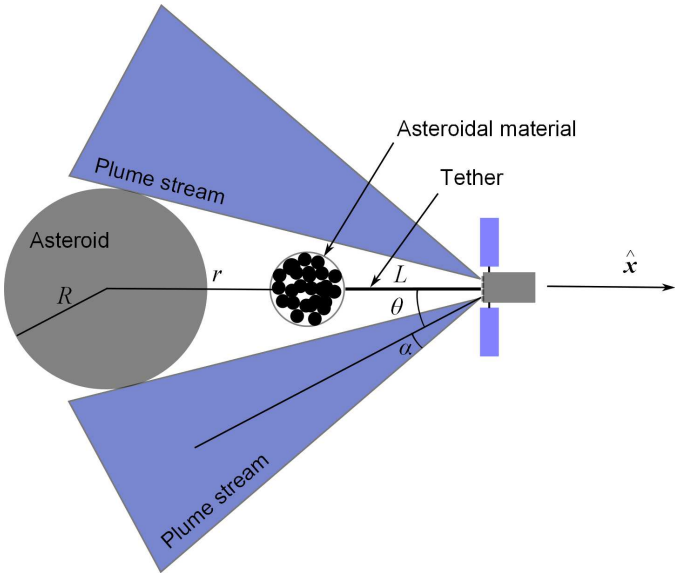

Figure 1: In-track EGT with a tether

II. In-Track EGT with Tether

One of the major disadvantages of the GT proposed by Lu and Love[13] is the thrust cant angle, which leads to an expenditure of propellant that does not directly contribute to deflecting the asteroid. The GT can be made more effective by moving the spacecraft closer to the asteroid to increase the gravitational attraction, but this increases the cant angle and, furthermore, reduces safety margin for the spacecraft. The cant angle can be made smaller by moving the spacecraft further away from the asteroid, but doing so reduces the gravitational attraction, and thus diminishes the effectiveness of the GT. If the spacecraft and the collected boulder mass are collocated, then the EGT is affected by the

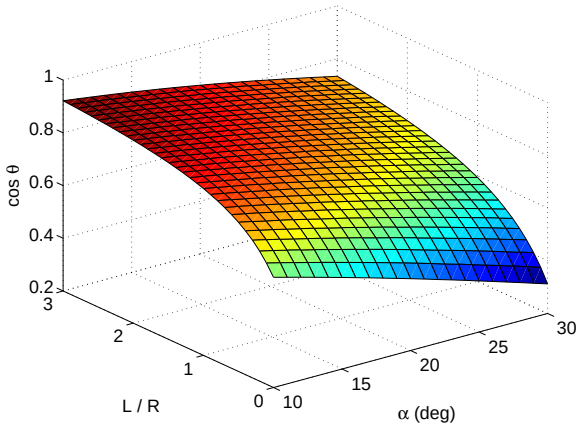

Figure 2: Thruster efficiency as a function of plume cone half-angle and tether length

same disadvantage. The dilemma can be avoided by furnishing the EGT with a tether. That is, the material collected from the asteroid is attached to a tether and placed where the EGT would have been without the tether, or even closer to the asteroid. With the asteroidal material on the tether, the spacecraft can be moved further away from the asteroid, as shown in Fig. 1, reducing the thruster cant angle and improving the safety margin for the spacecraft. The reduction in the cant angle varies, depending on the length of the tether and the distance from the asteroid to the asteroidal material. The asteroidal material obtained from the surface could be a single monolithic boulder, multiple boulders, or a collection of regolith; in this paper we will use the terms "asteroidal material" and "boulder" interchangeably.

In Fig. 1, $\hat{\mathbf{x}}$ is a unit vector that has the same direction as the velocity of the asteroid's mass center in heliocentric orbit; henceforth, this is referred to as the in-track direction. The asteroid is modeled as a sphere of radius R with uniform mass distribution. α denotes the half-angle of the plume cone, r is the distance from the collected material to the mass center of the asteroid, and L is the length of the tether. Thruster plumes will impinge on the asteroid if the thruster cant angle is below a minimum value, θ, given by

$$\theta = \sin^{-1}(R/d) + \alpha \tag{1}$$

where the distance d between the mass centers of the asteroid and the spacecraft is simply

$$d = r + L \tag{2}$$

The EGT thruster efficiency, the fraction of the thrust that directly contributes to deflecting the asteroid, is expressed as $\cos\theta$. An example of the thruster efficiency as a function of the tether length and cone half-angle is shown in Fig. 2, which is produced with $R = 100$ m and $r = 1.5R$, as in the paper by Lu and Love.[13] In Fig. 2, $L/R = 0$ corresponds to the case where the spacecraft and the asteroidal material are collocated. It can be seen that EGT thruster efficiency can be improved dramatically by increasing the length of the tether.

The magnitude of the gravitational force per unit of asteroid mass exerted by the boulder and the spacecraft on the asteroid is given by

$$\frac{F}{m_A} = G\left(\frac{m_B}{r^2} + \frac{m_C}{d^2}\right) \tag{3}$$

where G is the universal gravitational constant, m_A is the mass of the asteroid, m_B is the mass of the boulder, and m_C is the mass of the spacecraft. The associated velocity increment ΔV per year is obtained by multiplying F/m_A by 1 year, or 31,536,000 seconds. If we take $m_B = 0$, $m_C = 1000$ kg, $L = 0$, and $R = 160$ m (the radius of the asteroid Apophis), we find $\Delta V = 3.65 \times 10^{-5}$ m/s per year, in agreement with Fig. 2 in Ref. [18]. It is interesting to note that the right-hand member of the expression is independent of m_A; therefore, once a value for r is specified, the results are not necessarily limited to a particular asteroid, provided that the thrust limit is not reached. Figure 3 is obtained with $m_C = 8000$ kg and $r = 1.5R$. Clearly, if the collected boulders have at least as much mass as the spacecraft, the boulders compensate for the larger distance of the spacecraft as the tether length increases.

For present purposes the tether is regarded as a rigid rod with no mass. In future work we will consider the mass and elasticity of the tether in investigating the dynamics and control of the EGT. When the boulder is considered to

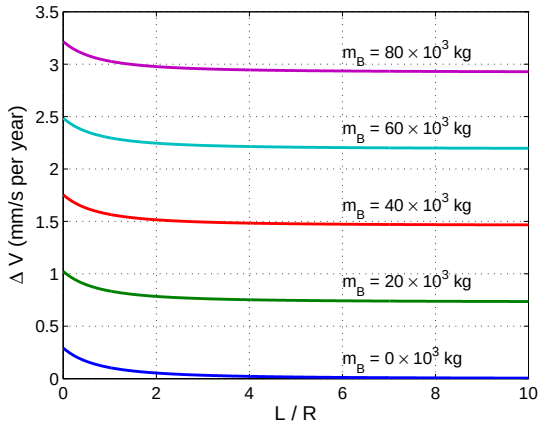

Figure 3: Yearly velocity increment as a function of boulder mass and tether length

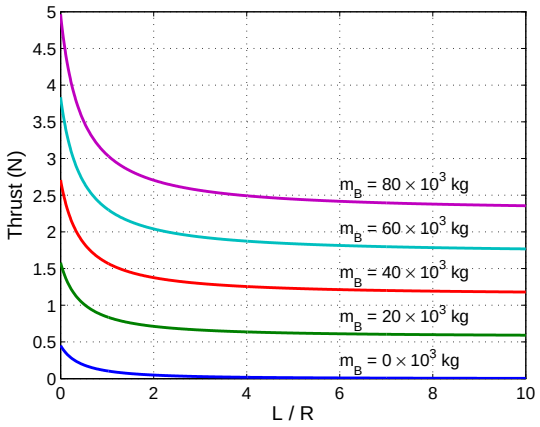

Figure 4: Thrust as a function of boulder mass and tether length

be in static equilibrium, the static tension in the tether is determined to be $Gm_B(m_A/r^2 - m_C/L^2)$. The spacecraft is subject to gravitational force exerted by the asteroid, gravitational force exerted by the boulder, tether tension, and thrust force. Lu and Love proposed two canted thrusters. In that case, the thrust force required from each of the two thrusters to place the spacecraft in a static equilibrium is given by

$$T = \frac{Gm_A}{2\cos\theta}\left(\frac{m_B}{r^2} + \frac{m_C}{d^2}\right) \tag{4}$$

The required thrust grows linearly with boulder mass. If we take $m_B = 0$, $m_C = 1000$ kg, $L = 0$, $\alpha = 20°$, and use the following values representative of Apophis, $R = 160$ m and $m_A = 4.6 \times 10^{10}$ kg, we obtain $T = 0.056$ N, in agreement with Fig. 2 in Ref. [18]. The results in Fig. 4 are produced with $m_C = 8000$ kg, $r = 1.5R$, and $\alpha = 20°$. The benefit of the tether in increasing the thruster efficiency and thereby reducing the required thrust becomes more pronounced as boulder mass increases.

An example of using a tether to improve the asteroid deflection will be shown next. Four fictitious spherical asteroids with diameters of 200 m, 300 m, 400 m, and 500 m and density of 2000 kg/m^3 are considered. Each asteroid is assumed to be in a circular heliocentric orbit with semi-major axis of 1 AU. It is assumed that the spacecraft dry mass is 4000 kg, and 5000 kg of propellant is available at the beginning of the EGT operation, all of which will be consumed to deflect an asteroid. Each of the two thrusters can produce a maximum thrust of 1 N at 1 AU, with specific impulse of 3000 s. The variation of the maximum thrust as a function of the heliocentric radius is neglected in this exercise. In addition, the distance r between the mass centers of the asteroid and boulder is to be kept close to but not less than $1.5R$.

For a value of $L/R = 10$, the distance r can be made approximately $1.5R$ and the required thrust can be kept below the limit of 2 N by selecting a particular boulder mass for each of the four asteroids, as indicated in Fig. 5. It can be seen that as tether length decreases, the boulder must be moved farther away from the asteroid to stay within the thrust limit. Figure 6 shows the amount of time it takes to exhaust the available propellant. As the propellant is expelled, the mass of the spacecraft decreases and thus the thrust required for the EGT also decreases. However, with a longer tether, the spacecraft is placed farther from the asteroid and thus the required thrust decreases at a slower rate. This causes the spacecraft to exhaust the available propellant faster, as shown in Fig. 6. Figure 6 also shows that for a given tether length, the time needed to exhaust the propellant increases with asteroid size.

Figures 7 and 8 show the deflection and ΔV at the time the propellant is completely spent, as well as the percentage improvement obtained by increasing L/R from 0 to 10. It can be seen that using a tether reduces the thrusting period, but increases the amount of deflection and thus improves the efficiency of the EGT operation. The improvement ranges from 28% to 37% for the deflection distance for the cases considered, and similar improvement is achieved for the ΔV. It should be noted that the deflection reported here is a result of integrating Hill's equations,[19] so the orbital amplification effect as reported in Ref. [15] is included in Figs. 7 and 8. When Hill's equations are solved with constant force per unit mass applied in the in-track direction, the in-track deflection for large values of the time t is a factor of three larger than the deflection that would occur in the case of one-dimensional rectilinear motion. The factor of 3 is referred to as orbital amplification.

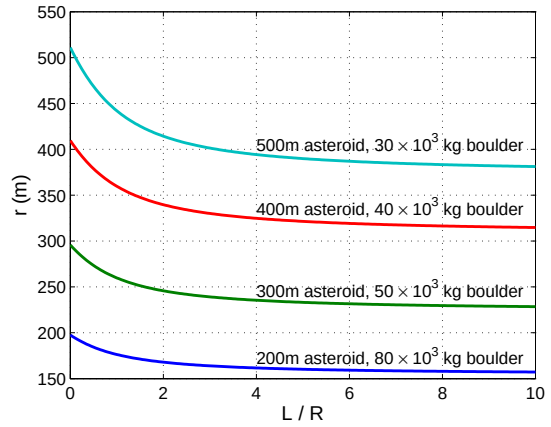

Figure 5: Distance from asteroid to boulder, and boulder mass, such that thrust limit of 2 N is met

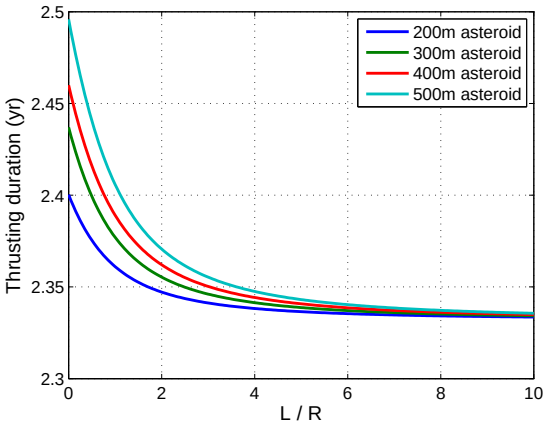

Figure 6: The duration of thrusting to exhaust 5,000 kg of propellant

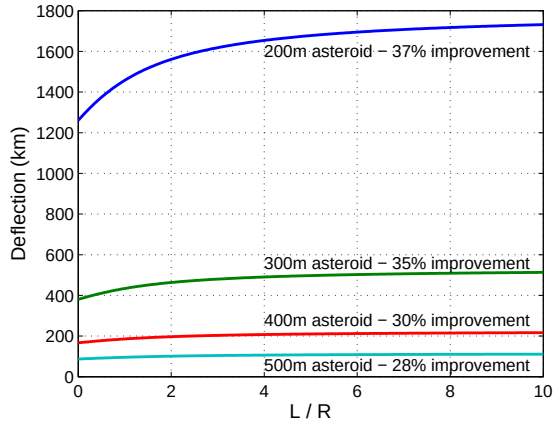

Figure 7: The deflection at the end of propellant depletion

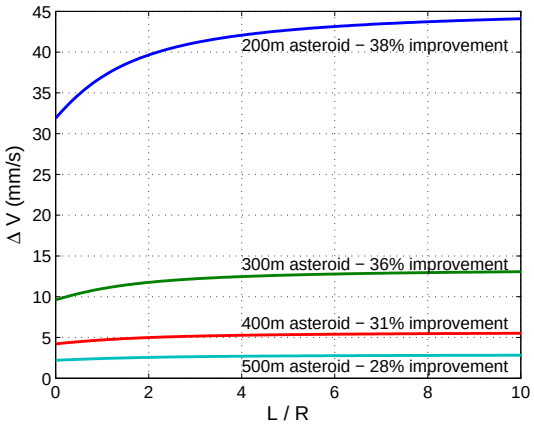

Figure 8: The ΔV at the end of propellant depletion

III. EGT with a Tether and Solar Sail

The reduction in thruster efficiency caused by canting the thrust direction, as is necessary for Lu and Love's gravity tractor as well as the tractor considered in Sec. II, can be eliminated by placing the spacecraft in the plane of the asteroid's heliocentric orbit, slightly farther away from the Sun than the asteroid, so that the exhaust plume does not impinge on the asteroid. A static radial displacement can be achieved by means of a solar sail, as illustrated in Fig. 9.

The angle θ, which previously denoted a thruster cant angle, can instead be regarded as the angle between the axis of symmetry of a single plume cone (parallel to the asteroid's in-track direction) and the tether that is parallel to local vertical at the spacecraft's mass center. The angle is referred to as "offset angle" in Ref. [15]. The relationship for θ in Eq. (1) remains valid.

Two relationships are obtained by requiring a zero resultant of forces acting on the spacecraft: propulsive thrust, solar radiation pressure force, gravitational force exerted by the asteroid, gravitational force exerted by the boulder, and tether tension.

$$T - Gm_A\left(\frac{m_B}{r^2} + \frac{m_C}{d^2}\right)\cos\theta + 2PA\cos^2\beta\sin\beta = 0 \tag{5}$$

$$Gm_A\left(\frac{m_B}{r^2} + \frac{m_C}{d^2}\right)\sin\theta - 2PA\cos^2\beta\cos\beta = 0 \tag{6}$$

where T is propulsive thrust force, A is the area of the solar sail, and P is the solar radiation pressure constant at 1

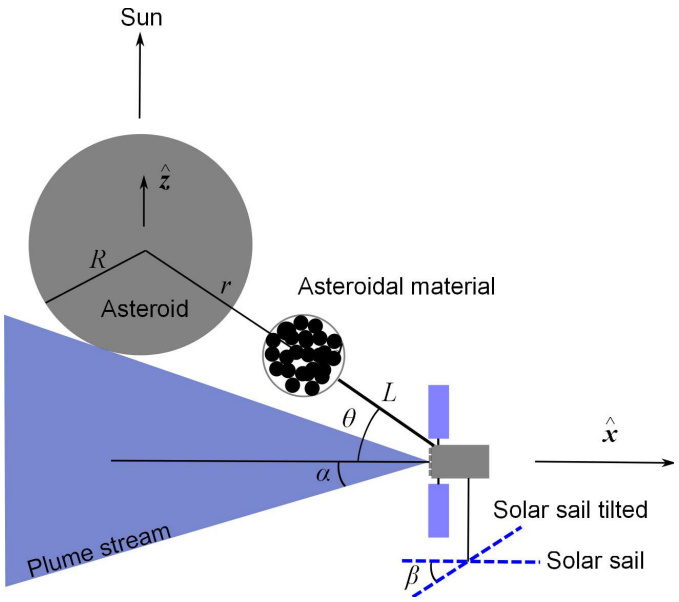

Figure 9: Offset EGT with a tether and solar sail

A.U., $P = 4.5 \times 10^{-6}$ N/m^2. Here, we assume that the spacecraft has a heliocentric distance of 1 A.U., and reflection of solar radiation by the sail is completely specular. β is the angle between a unit vector normal to the plane of the solar sail (on the side facing away from the Sun), and $-\hat{\mathbf{z}}$, where $\hat{\mathbf{z}}$ is a unit vector that has the same direction as the position vector from the asteroid's mass center to the Sun's mass center. With specified values for m_A, m_B, m_C, r, L, α, and β, one can use Eq. (6) to determine the required sail area A, and then use Eq. (5) to obtain the necessary propulsive thrust. Substitution from Eq. (6) into (5) yields

$$T = Gm_A \left(\frac{m_B}{r^2} + \frac{m_C}{d^2} \right) (\cos\theta - \sin\theta \tan\beta) \tag{7}$$

Hence, for $\beta \neq 0$, T vanishes when $\beta = \beta^* = \tan^{-1}(\cos\theta / \sin\theta)$. For $\beta > \beta^*$, the spacecraft will escape the asteroid.

Henceforth, the solar sail is assumed to be square in shape, and the length of a side is simply $s = \sqrt{A}$. If the solar sail is to remain fully illuminated, there is a limit to how large s can be. With the aid of Fig. 9, one can express the condition that no part of the solar sail is eclipsed by the asteroid.

$$\frac{s}{2} \cos\beta \leq d\cos\theta - R \tag{8}$$

The magnitude of the gravitational force per unit of asteroid mass exerted by the boulder and the spacecraft on the asteroid in the in-track direction is given by

$$\frac{F}{m_A} = G \left(\frac{m_B}{r^2} + \frac{m_C}{d^2} \right) \cos\theta \tag{9}$$

As explained in Ref. [15], the force per unit mass applied to the asteroid in a direction parallel to $\hat{\mathbf{z}}$ has a negligible effect on asteroid deflection. Thus, the decrease in deflection efficiency of a gravity tractor with increasing offset angle is analogous to the decrease in thruster efficiency with increasing cant angle in the case of an in-track gravity tractor. The velocity increment ΔV associated with in-track deflection is obtained by multiplying F/m_A in Eq. (9) by the amount of time spent towing the asteroid with the gravity tractor; for a long period of towing, an orbital amplification factor of 3 is applied, as discussed in Ref. [15].

The results that follow are obtained with $m_A = 4.6 \times 10^{10}$ kg, $m_C = 8000$ kg, $R = 160$ m, $r = 1.5R$, and $\alpha = 20°$. The critical tilt angle β^*, at which no propulsive thrust is needed, is plotted as a function of L/R in Fig. 10. The solar sail dimension s required for tilt angle β^* is plotted in Fig. 11 as a function of L/R for several values of boulder mass. Each curve is displayed over the range of L/R in which s satisfies Eq. (8) and the sail therefore is fully illuminated. Some portion of the solar sail is in shadow to the left of the boundary marked by the dashed curve.

The required propulsive thrust and sail dimension s with $\beta = 0$ are shown as functions of L/R, for several values of m_B, in Figs. 12 and 13 respectively, where the dashed curves have the same meaning as in Fig. 11. For a given value of boulder mass, the dimension of the untilted sail in Fig. 13 is significantly smaller than the dimension of the fully tilted sail in Fig. 11; the reduction in sail size is purchased with the thrust levels displayed in Fig. 12.

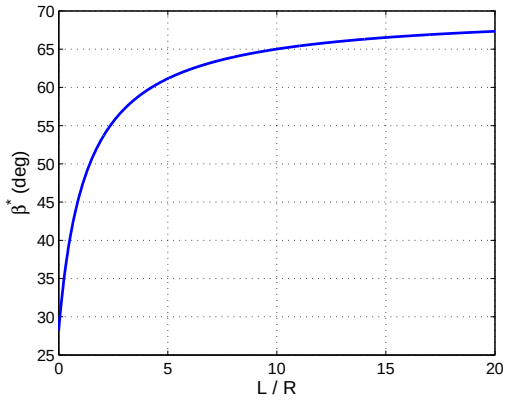

Figure 10: Sail tilt angle β^* at which EGT requires no propulsive thrust

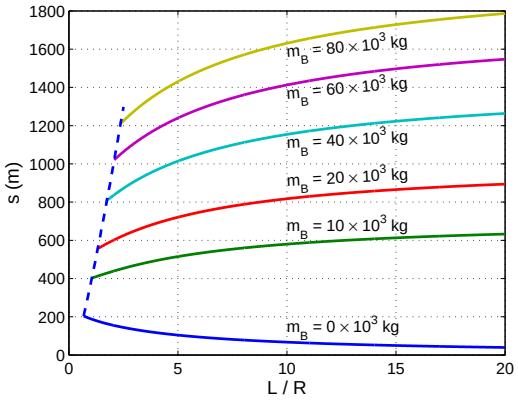

Figure 11: Required size of the solar sail tilted by angle β^*

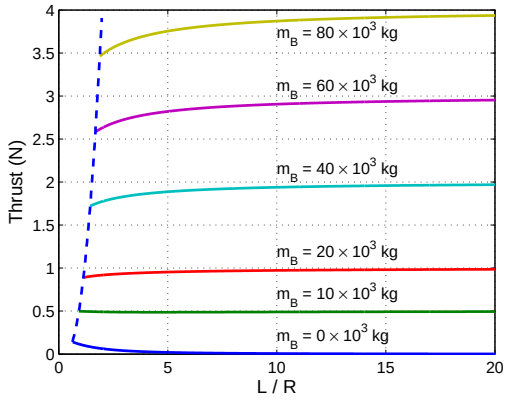

Figure 12: Thrust as a function of boulder mass and tether length, $\beta = 0°$

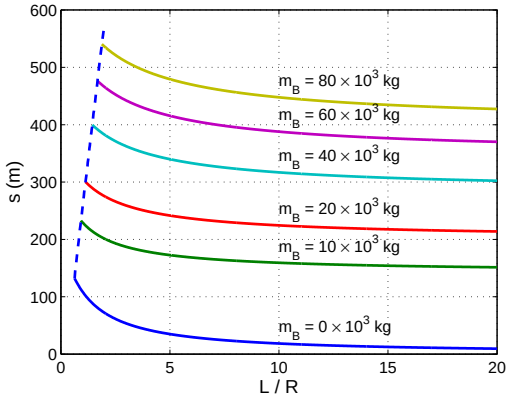

Figure 13: Solar sail size as a function of boulder mass and tether length, $\beta = 0°$

IV. Multiple EGTs with Tethers and Solar Sails

Deploying multiple EGTs rather than a single spacecraft can reduce the amount of time needed to apply a given ΔV to an asteroid, or increase the amount of ΔV imparted during a given time interval. However, it is imperative that the EGTs be well separated spatially so that they don't collide with each other. Here we propose a scheme that is an extension of the one introduced in Sec. III. Two additional spacecraft, each furnished with a tether and a solar sail, can be placed on either side of the asteroid's heliocentric orbit plane; in this case, their solar sails can be oriented so as to maintain the out-of-plane positions. All three spacecraft are in front of the asteroid. The situation is illustrated in Fig. 14, where the asteroid is viewed from behind. The unit vector $\hat{\mathbf{y}}$ is normal to the asteroid's heliocentric orbit plane. Placing multiple EGTs with tethered masses on a halo orbit is operationally challenging because of the risk of the tethers getting tangled up. However, because the EGTs in Fig. 14 operate at static equilibria, the risk of tangling tethers is mitigated.

The EGT on the bottom of Fig. 14 functions exactly as described in Sec. III, so here we focus on the out-of-plane spacecraft on the left. It is assumed that each EGT is displaced out of the asteroid's orbit plane just enough to prevent the plume cone from impinging on the asteroid (see Fig. 9). Thus, the offset angle θ is again given by Eq. (1). The angles γ and λ are described as follows. With the plane of the solar sail initially parallel to the plane containing $\hat{\mathbf{x}}$ and

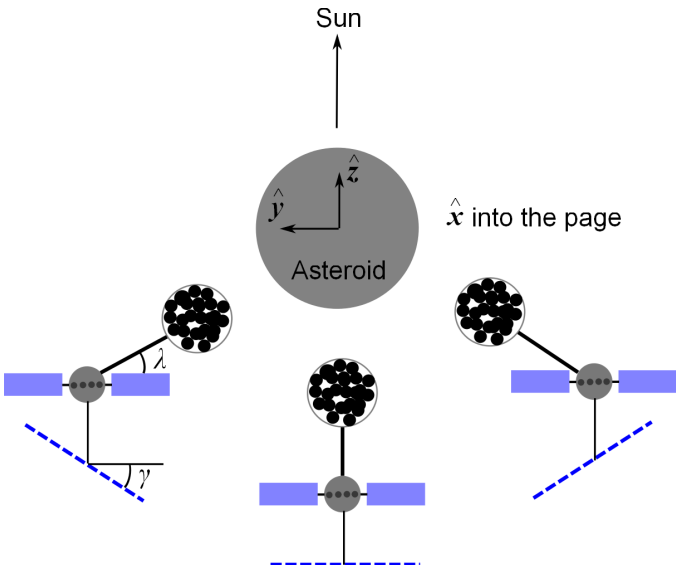

Figure 14: Three EGTs with tethers and solar sails

$\hat{\mathbf{y}}$, the solar sail is rotated about $\hat{\mathbf{x}}$ by an amount γ. Hence, γ is the angle between a unit vector normal to the plane of the solar sail (on the side facing away from the Sun) and $-\hat{\mathbf{z}}$, such that the spacecraft is in equilibrium. As for the angle λ, consider a set of right-handed, mutually orthogonal unit vectors $\hat{\mathbf{r}}$, $\hat{\mathbf{s}}$, and $\hat{\mathbf{t}}$ that initially have the same directions as $\hat{\mathbf{x}}$, $\hat{\mathbf{y}}$, and $\hat{\mathbf{z}}$, respectively. Subject the reference frame in which $\hat{\mathbf{r}}$, $\hat{\mathbf{s}}$, and $\hat{\mathbf{t}}$ are fixed to successive rotations, first about $\hat{\mathbf{r}}$ in the amount $-\lambda$ and then about $\hat{\mathbf{t}}$ in the amount θ. The unit vector $\hat{\mathbf{r}}$ thus obtained has the same direction as the position vector from the asteroid's mass center to the spacecraft's mass center, and is parallel to the tether.

The conditions under which the solar sail is not eclipsed by the asteroid can be obtained with the aid of Fig. 15. Assume that the spacecraft is mounted at the center of the solar sail, denoted as point C. Let the corner of the solar sail on the rear edge toward the $-\hat{\mathbf{y}}$ direction be denoted by point D. Then $\mathbf{r}^{OD}$, the position vector from O, the center of the asteroid, to point D, can be written as

$$\begin{aligned}\mathbf{r}^{OD} &= \mathbf{r}^{OC} + \mathbf{r}^{CD} \\ &= \left(d\cos\theta - \frac{s}{2}\right)\hat{\mathbf{x}} + \left(d\cos\lambda\sin\theta - \frac{s}{2}\cos\gamma\right)\hat{\mathbf{y}} - \left(d\sin\lambda\sin\theta + \frac{s}{2}\sin\gamma\right)\hat{\mathbf{z}} \\ &\triangleq x_D\hat{\mathbf{x}} + y_D\hat{\mathbf{y}} + z_D\hat{\mathbf{z}}\end{aligned} \tag{10}$$

The conditions for full illumination of the sail can be readily deduced by considering the projections of the sail and the asteroid onto the $\hat{\mathbf{x}}$-$\hat{\mathbf{y}}$ plane. Because propulsive thrust is to be applied in the direction of $\hat{\mathbf{x}}$ and solar radiation pressure force is to be applied in the direction of $\hat{\mathbf{y}}$, the sail center C must remain in the first quadrant of the $\hat{\mathbf{x}}$-$\hat{\mathbf{y}}$ plane. Sail corner D can be in one of three quadrants, as illustrated in Figs. 15(b)–15(d). For each of the three possibilities, a condition for full illumination can be expressed in terms of x_D and y_D, the measure numbers of $\mathbf{r}^{OD}$ for unit vectors $\hat{\mathbf{x}}$ and $\hat{\mathbf{y}}$ [see Eq. (10)].

$$\begin{cases} \sqrt{x_D^2 + y_D^2} \geq R, & \text{when } x_D \geq 0 \text{ and } y_D \geq 0 \quad (D \text{ in } 1^{\text{st}} \text{ quadrant}) \\ y_D \geq R, & \text{when } x_D \leq 0 \text{ and } y_D \geq 0 \quad (D \text{ in } 2^{\text{nd}} \text{ quadrant}) \\ x_D \geq R, & \text{when } x_D \geq 0 \text{ and } y_D \leq 0 \quad (D \text{ in } 4^{\text{th}} \text{ quadrant}) \end{cases} \tag{11}$$

It is clear that when point D appears in the 3^{rd} quadrant of the $\hat{\mathbf{x}}$-$\hat{\mathbf{y}}$ plane, the solar sail is definitely eclipsed by the asteroid.

The equilibrium of the spacecraft at the bottom of Fig. 14 is analyzed in Section III. For the spacecraft on the left side, three relationships are obtained by requiring a zero resultant of forces acting on the spacecraft: propulsive thrust, solar radiation pressure force, gravitational force exerted by the asteroid, gravitational force exerted by the boulder,

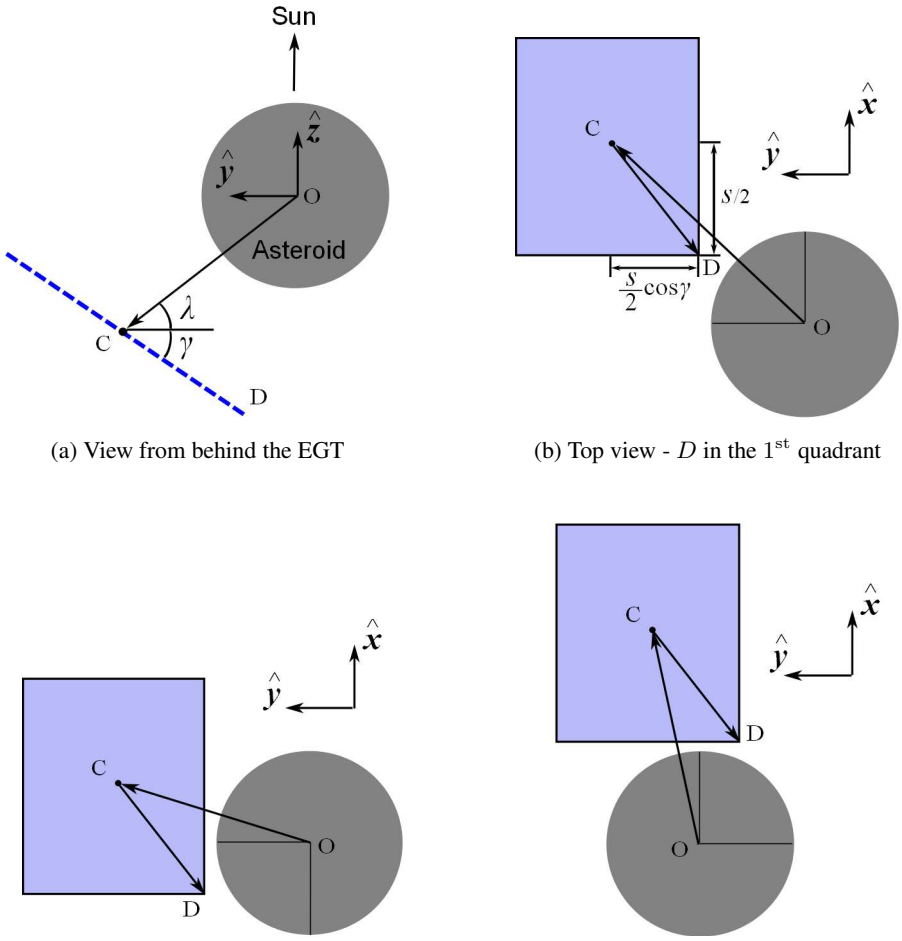

(a) View from behind the EGT

(b) Top view - D in the 1^{st} quadrant

(c) Top view - D in the 2^{nd} quadrant

(d) Top view - D in the 4^{th} quadrant

Figure 15: Illustration of shadow conditions for the solar sail on the left side

and tether tension.

$$T - Gm_A\left(\frac{m_B}{r^2} + \frac{m_C}{d^2}\right)\cos\theta = 0 \tag{12}$$

$$Gm_A\left(\frac{m_B}{r^2} + \frac{m_C}{d^2}\right)\sin\theta\cos\lambda - 2PA\cos^2\gamma\sin\gamma = 0 \tag{13}$$

$$Gm_A\left(\frac{m_B}{r^2} + \frac{m_C}{d^2}\right)\sin\theta\sin\lambda - 2PA\cos^2\gamma\cos\gamma = 0 \tag{14}$$

One can use Eq. (12) to obtain the necessary propulsive thrust. Equations (13) and (14) yield

$$Gm_A\left(\frac{m_B}{r^2} + \frac{m_C}{d^2}\right)\sin\theta = 2PA\cos^2\gamma \tag{15}$$

$$\tan\lambda = \cot\gamma \tag{16}$$

In obtaining Eq. (15) it is worth noting the identity $\tan x = \cot(\pi/2 - x)$; thus, Eq. (16) implies $\lambda + \gamma = \pi/2$ and, consequently, $\sin\lambda = \cos\gamma$ and $\cos\lambda = \sin\gamma$. One can use Eq. (15) to calculate the necessary size of the solar sail, given a tilt angle γ, and use Eq. (16) to obtain λ, which along with θ and d determines the position of the spacecraft at the equilibrium.

The results that follow are obtained with $m_A = 4.6 \times 10^{10}$ kg, $m_C = 8000$ kg, $R = 160$ m, $r = 1.5R$, and $\alpha = 20°$.

The required dimension s of the side sail, and the minimum distance between a side sail and the bottom sail (see Fig. 14), is presented in Fig. 16 for side sail tilt angle in the range $0 \leq \gamma \leq 80°$, $L/R = 5$, 10, 15, and 20, and four

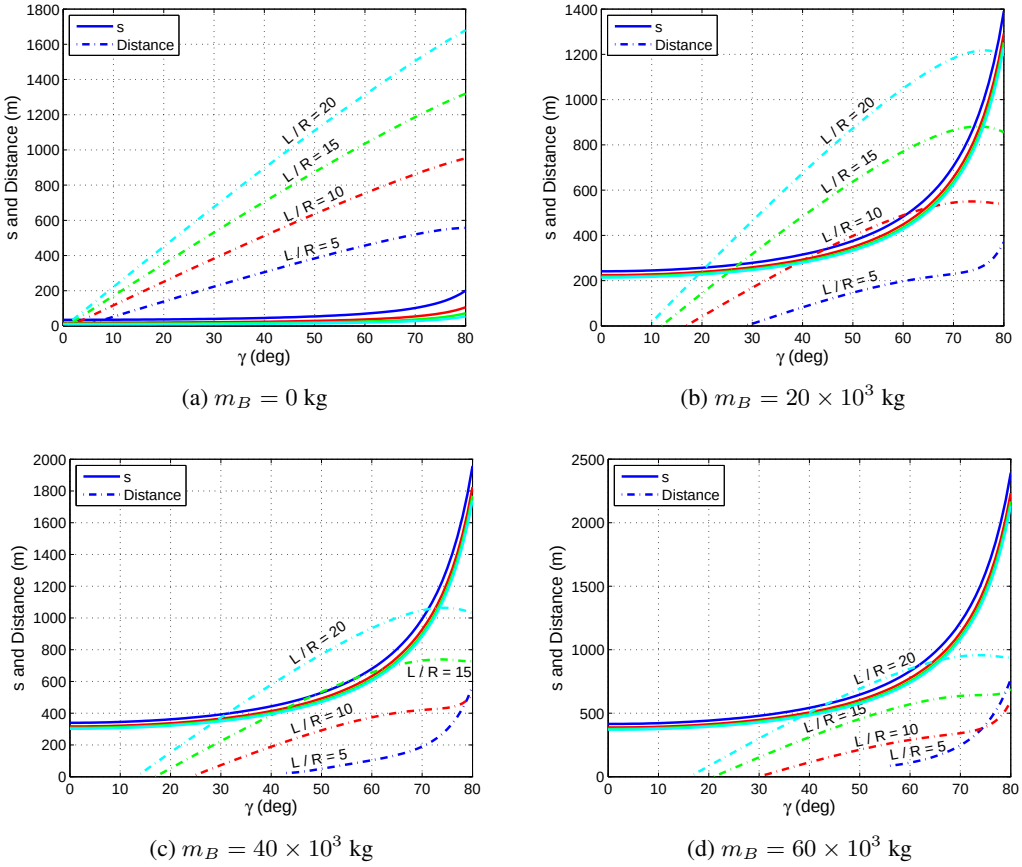

(a) $m_B = 0$ kg

(b) $m_B = 20 \times 10^3$ kg

(c) $m_B = 40 \times 10^3$ kg

(d) $m_B = 60 \times 10^3$ kg

Figure 16: Required size of side sail, and minimum distance between side sail and bottom sail

values of boulder mass, $m_B = 0$, 20×10^3, 40×10^3, and 60×10^3 kg. The side and bottom sails are attached to EGTs employing tethers presumed to have equal lengths. Curves for s are solid, whereas dash-dot curves are used to show minimum distance. Curves corresponding to $L/R = 5$, 10, 15, and 20 are colored blue, red, green, and light blue, respectively. As boulder mass and sail size increase, higher values of tilt angle γ are required to prevent the bottom sail from casting a shadow on the side sail. Higher values of γ are required as tether length decreases, for the same reason. The curves of minimum distance are not shown for values of γ for which one of the following three eclipse conditions occurs: 1) the bottom sail is eclipsed by the asteroid, 2) the side sail is eclipsed by the asteroid, and 3) the side sail is in the shadow of the bottom sail. For example, in Fig. 16d, the curve for minimum distance with $L/R = 5$ is not displayed for $\gamma < 55^\circ$ because the side sail enters the shadow of the bottom sail for lower values of γ. However, large values of γ are to be avoided because required sail area becomes large and, as discussed in what follows immediately, the solar radiation pressure force in the $\hat{\mathbf{y}}$ direction becomes small.

The magnitude of the solar radiation pressure force in the $\hat{\mathbf{y}}$ direction involves the term $\cos^2\gamma \sin\gamma$, as may be seen in Eq. (13), and this term is maximum at $\gamma = 35^\circ$. For this value of γ, the required dimension s of a square solar sail is shown in Fig. 17. As boulder mass increases, the side sail must get larger; for a given boulder mass, the sail size decreases as the tether becomes longer. Some portion of the solar sail is eclipsed by the asteroid, in the region to the left of the boundary marked by the dashed curve. The minimum distance between the two side sails attached to EGTs employing tethers with equal lengths is shown in Fig. 18. With the exception of the case with $m_B = 0$, the tether length cannot be reduced to zero because this will result in the two side sails coming into contact with each other. The minimum distance between a side sail and the bottom sail (see Fig. 14), when they are attached to spacecraft having tethers of equal lengths, is shown in Fig. 19. The dashed curve again marks a boundary at which the side sail enters the shade of the bottom sail. It can be seen in Figs. 18 and 19 that when all three tethers are of the same length, healthy sail separation can be achieved only with longer tethers, especially in the cases of more massive boulders. Alternatively, tethers on the side and bottom EGTs can be given different lengths to avoid interference between solar sails, particularly for the smaller tether lengths. The clearance between side and bottom sails with different tether

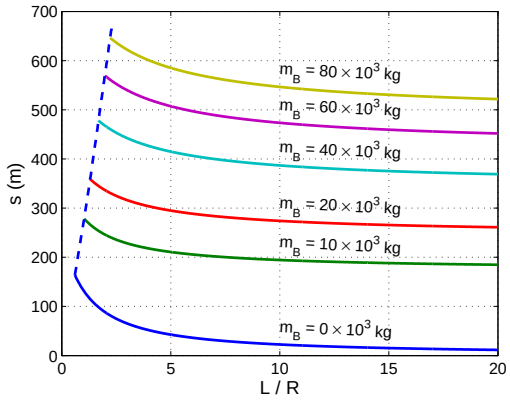

Figure 17: Required size of the side solar sails with $\gamma = 35°$

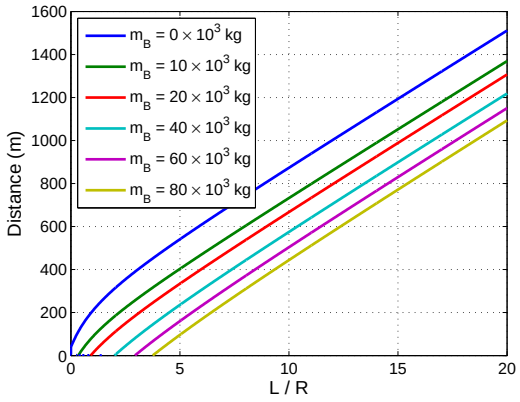

Figure 18: Distance between the two side sails with the same tether length and $\gamma = 35°$

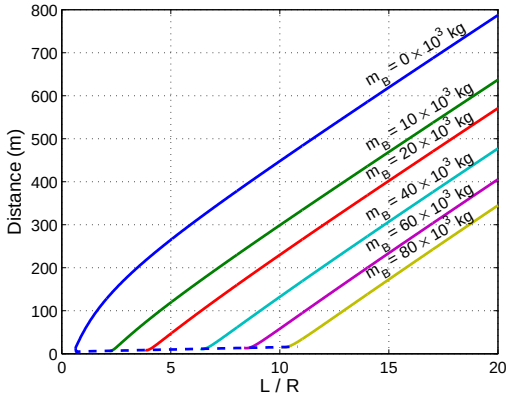

Figure 19: Distance between the side and bottom sails with the same tether length and $\gamma = 35°$

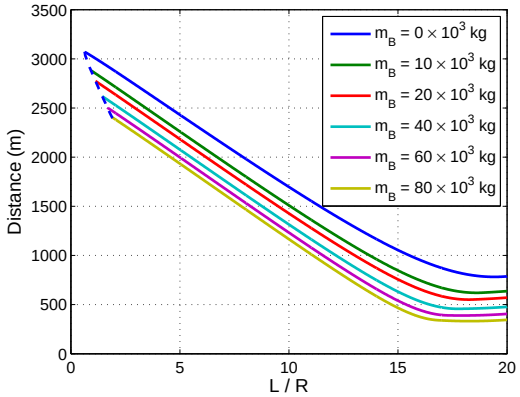

Figure 20: Distance between the side and bottom sails with the side sail at $L/R = 20$ and $\gamma = 35°$

lengths is illustrated in Fig. 20, where the value of L/R is fixed at 20 for the side sail and allowed to vary for the bottom sail. Some portion of the bottom sail is eclipsed by the asteroid, in the region to the left of the boundary marked by the dashed curve. Clearly, sail separation is improved by making the tether lengths different.

V. Conclusions

Three new enhanced gravity tractor concepts are presented in this paper, utilizing tethers and solar sails. The first concept uses a tether to improve the thruster efficiency of an in-track gravity tractor. With a tether, the asteroidal material picked up from the asteroid surface is placed close to the asteroid while the spacecraft can be kept farther away to reduce the thruster cant angle and improve the safety margin for the spacecraft. Numerical examples show that for the same amount of propellant, using a tether results in improved deflection within a shorter time period compared to the case where the spacecraft and the asteroidal material are collocated. The second concept utilizes a solar sail to offset the spacecraft radially so that the thruster plume stream does not impinge on the asteroid surface. A tether is used to the same advantage as in the first concept: it permits collected asteroidal material to be close to the asteroid and the spacecraft to be farther away. The required sail size and thrust are analyzed for a range of tether lengths and collected masses. The spacecraft proposed in the second concept is augmented in the third concept with two similar spacecraft, one of which is placed on each side of the first spacecraft. Spatial separation of the EGTs can be achieved by tilting the two side sails about the in-track direction. The sizes of the solar sails and the distances between the sails are analyzed for a range of tether lengths and masses of asteroidal material, while accounting for eclipse of the sails by the asteroid and other sails. These concepts have the potential to increase the effectiveness of enhanced gravity tractors, should it be necessary to deflect an asteroid to prevent it from colliding with Earth.

References

[1]Küppers, M., et al., "Boulders on Lutetia," *Planetary and Space Science*, Vol. 66, No. 1, 2012, pp. 71–78, Doi:10.1016/j.pss.2011.11.004.

[2]Veverka, J., et al., "The Landing of the NEAR-Shoemaker Spacecraft on Asteroid 433 Eros," *Nature*, Vol. 413, September 2001, pp. 390–393, Doi:10.1038/35096507.

[3]Thomas, P. C., Veverka, J., Robinson, M., and Murchie, S., "Shoemaker Crater as the Source of Most Ejecta Blocks on the Asteroid 433 Eros," *Nature*, Vol. 413, September 2001, pp. 394–396, Doi:10.1038/35096513.

[4]Lewis, J. S., *Rain of Iron and Ice: The Very Real Threat of Comet and Asteroid Bombardment*, Helix Books, Addison-Wesley Publishing Company, Inc., 1996.

[5]Friedman, G., "The increasing recognition of near-Earth-objects (NEOs)," Space Manufacturing 10: Pathways to the High Frontier, Proceedings of the Twelvth SSI-Princeton Conference, 4-7 May 1995, edited by Barbara Faughnan, AIAA, pages 157-164.

[6]Chesley, S. and Ward, S., "Quantitative Assessment of Human Economic Hazards from Impact-Generated Tsunami," *Natural Hazards*, Vol. 38, No. 3.

[7]Popova, O. P., et al., "Chelyabinsk Airburst, Damage Assessment, Meteorite Recovery, and Characterization," *Science*, Vol. 342, No. 6162, pp. 1069–1073, Doi: 10.1126/science.1242642.

[8]McInnes, C. R., "Deflection of Near-Earth Asteroids by Kinetic Energy Impacts from Retrograde Orbits," *Planetary and Space Science*, Vol. 52, No. 7, 2004, pp. 587–590, Doi: 10.1016/j.pss.2003.12.010.

[9]Wie, B., "Solar Sailing Kinetic Energy Interceptor Mission for Impacting and Deflecting Near-Earth Asteroids," The 41st AIAA Joint Propulsion Conference and Exhibit, AIAA Paper 2005-3725, Tucson, AZ, July 2005.

[10]Dachwald, B. and Wie, B., "Solar Sail Kinetic Energy Impactor Trajectory Optimization for an Asteroid-Deflection Mission," *Journal of Spacecraft and Rockets*, Vol. 44, No. 4, 2007, pp. 755–764, Doi: 10.2514/1.22586.

[11]Ahrens, T. J. and Harris, A. W., "Deflection and fragmentation of near-Earth asteroids," *Nature*, Vol. 360, December 1992, pp. 429–433, Doi: 10.1038/360429a0.

[12]Bombardelli, C. and Pelaez, J., "Ion Beam Shepherd for Asteroid Deflection," *Journal of Guidance, Control, and Dynamics*, Vol. 34, No. 4, 2011, pp. 1270–1272, Doi: 10.2514/1.51640.

[13]Lu, E. T. and Love, S. S., "Gravitational Tractor for Towing Asteroids," *Nature*, Vol. 438, Nov. 2005, pp. 177–178, Doi: 10.1038/438177a.

[14]McInnes, C. R., "Near Earth Object Orbit Modification Using Gravitational Coupling," *Journal of Guidance, Control, and Dynamics*, Vol. 30, No. 3, 2007, pp. 870–873, Doi: 10.2514/1.25864.

[15]Wie, B., "Dynamics and Control of Gravity Tractor Spacecraft for Asteroid Deflection," *Journal of Guidance, Control, and Dynamics*, Vol. 31, No. 5, 2008, pp. 1413–1423, Doi: 10.2514/1.32735.

[16]Mazanek, D. D., Merrill, R. G., Belbin, S. P., Reeves, D. M., Naasz, B. J., Abell, P. A., and Earle, K., "Asteroid Redirect Robotic Mission: Alternate Concept Overview," AIAA SPACE 2014 Conference and Exposition, Aug. 4-7, 2014, San Diego, CA.

[17]Mazanek, D. D., Reeves, D. M., Hopkins, J. B., Wade, D. W., Tantardini, M., and Shen, H., "Enhanced Gravity Tractor Technique for Planetary Defense," 4th IAA Planetary Defense Conference - PDC 2015, 13-17 April 2015, Frascati, Roma, Italy.

[18]Schweickart, R., Chapman, C., Durda, D., and Hut, P., "Threat Mitigation: The Gravity Tractor," Tech. rep., B612 Foundation, White Paper 042, Sonoma, CA, June 2006.

[19]Kaplan, M. H., *Modern Spacecraft Dynamics and Control*, John Wiley & Sons, New York, 1976, p. 111.